

# Virgo: Cluster-level Matrix Unit Integration in GPUs for Scalability and Energy Efficiency

Hansung Kim\*, Ruohan Yan\*, Joshua You, Tieliang Vamber Yang, Yakun Sophia Shao

University of California, Berkeley

{hansung\_kim,yrh,jyou12,vamber,ysshao}@berkeley.edu

## Abstract

Modern GPUs incorporate specialized matrix units such as Tensor Cores to accelerate GEMM operations central to deep learning workloads. However, existing matrix unit designs are tightly coupled to the SIMT core, limiting the size and energy efficiency of the operation due to capacity and bandwidth constraints from the register file. Such a limitation in scalability makes it difficult to simultaneously enhance compute throughput and improve energy efficiency in GPUs.

To address this challenge, we propose *Virgo*, a new GPU microarchitecture that integrates dedicated matrix units at the *SIMT core cluster* level. By physically disaggregating the matrix unit from the SIMT core, Virgo eliminates scalability constraints imposed by the core microarchitecture. Consequently, Virgo increases the granularity of operations at the hardware which not only improves data reuse, but also reduces the number of instructions processed in the SIMT core. This reduction in instruction processing decreases energy consumption within the core pipeline, thereby improving the system-level energy efficiency. Our evaluations, implemented in synthesizable RTL, demonstrate that Virgo achieves up to 66.3% reduction in active power and 77.2% reduction in active energy consumption of the system-on-chip compared to the baseline core-coupled design.

## 1 Introduction

In recent years, the computational capability of GPUs has surged at an unprecedented rate, driven by the demand of emerging large-scale deep learning applications such as large language models [6, 15, 34]. To better meet these application demands, modern GPU architectures have increasingly incorporated specialized matrix units, such as NVIDIA Tensor Cores [8] and AMD Matrix Cores [1]. These units accelerate GEMM operations in deep learning workloads with significantly higher compute efficiency than the traditional general-purpose SIMD units.

As the demand for higher compute capabilities to grow, so too has the scale of integration of dedicated matrix units: the number of FLOPS achieved by Tensor Cores has increased eight-fold from Volta to Hopper, over the past five years [8, 11]. Beyond FLOPS, power and energy have become increasingly important for modern GPU workloads.

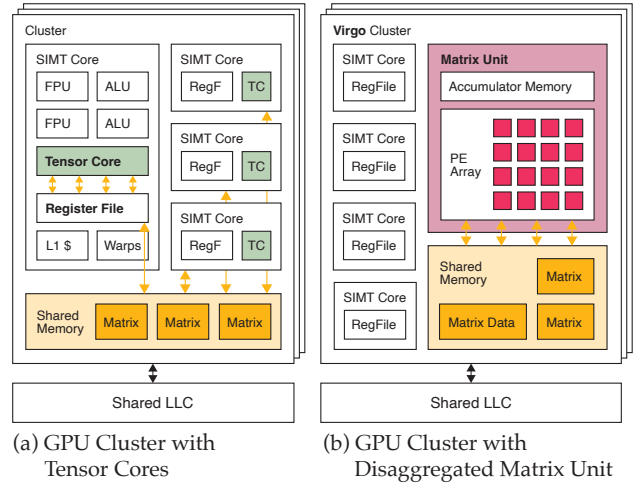


**Figure 1.** Overview of (a) today’s GPU architecture with tightly coupled integration of Tensor Cores (TC), compared to (b) Virgo’s cluster-level integration of matrix units.

Deep learning applications are known to be highly energy-intensive workloads on GPUs [21]. Moreover, GPUs are also often power-limited; datacenters frequently over-provision GPU resources, leading to frequent throttling to meet the power budget, which in turn compromises performance [5, 28–30, 45].

However, it is increasingly challenging to simultaneously meet the demand for higher FLOPS and better energy efficiency, due to the *tight coupling* between the matrix units and the GPU SIMT cores. Matrix units are typically integrated into the SIMT core pipeline as specialized functional units, receiving data through the register file via the standard instruction datapath. This tightly coupled integration faces significant limitations due to the capacity and bandwidth constraints of the register file. Furthermore, these core-coupled matrix units are designed to support fine-grained operations, commonly with tile sizes such as  $16 \times 8 \times 16$  [33, 36]. Such a small granularity of operation requires processing a large number of instructions in the core pipeline, consuming substantial energy and power in instruction decoding and scheduling, rather than in actual computation.

To address these challenges, we propose Virgo, a novel GPU architecture that integrates dedicated matrix units at the *cluster* level (Figure 1). The cornerstone of Virgo is the

\* These authors contributed equally to this work.

physical disaggregation of the matrix unit from the core microarchitecture, thereby eliminating scalability constraints. As a result, Virgo not only increases the operation granularity at the matrix unit, leading to greater data reuse and boosting energy efficiency, but it also cuts down the number of instructions processed by the SIMT core, lowering the overall system-level energy. We summarize the key contribution of our work as follows:

- We propose a novel cluster-level matrix unit integration methodology for GPUs that enhances scalability and efficiency by disaggregating the accelerator from the SIMT core.
- We fully implement GPU designs featuring both the proposed cluster-level integration and the baseline core-coupled integration in synthesizable RTL. We also develop the corresponding software programming interface leveraging the RISC-V ISA. The entire Virgo design will be made available as open source.
- We demonstrate that Virgo, synthesized using a commercial 16nm process, significantly improves active SoC power consumption by 66.3% and energy by 77.2%, compared to the core-coupled baseline.

## 2 Background and Motivation

This section provides an overview of the GPU and Tensor Core microarchitectures, highlighting the scalability and efficiency limitations caused by the tight coupling of the matrix unit to the SIMT core. This discussion motivates Virgo’s key design decision to integrate matrix units at the cluster level, addressing architectural bottlenecks and aligning with the increasing demands of modern GPU applications.

### 2.1 GPU Cluster Microarchitecture

Figure 1(a) shows the modern GPU microarchitecture, featuring multiple clusters of SIMT cores connected to a shared last-level cache. Each SIMT core consists of a warp scheduler, a register file, and tightly-coupled execution units like Tensor Cores. Within each cluster, SIMT cores are interconnected via a cluster-level network-on-chip to the *shared memory*, a software-managed scratchpad. The cluster-based architecture in GPUs is widely adopted in the industry, known as *Streaming Multiprocessors* in NVIDIA GPUs [11], *Compute Units* in AMD CDNA architecture [1] and *X<sup>e</sup>-cores* in Intel X<sup>e</sup>-HPG architecture [23].

The clustered organization offers several benefits. First, it increases warp-level parallelism by enabling multiple warps to execute simultaneously through the multiple cores in the cluster. Second, and more importantly, it enables increased data sharing between the threads. A cluster serves as the hardware unit to which a *thread block* or a *workgroup* is assigned. The SIMT threads in the same thread block can share data and synchronize across each other through the shared

GPU	V100	A100	H100
Architecture	Volta	Ampere	Hopper
Tensor FP16 TFLOPS	1x	2.5x	7.9x
CUDA FP32 TFLOPS	1x	1.2x	4.3x
# of Tensor Cores	1x	0.7x	0.8x
MACs in 1 Tensor Core	<b>64</b>	<b>256</b>	<b>473</b>
Registers per thread (max. 255)	224	221	168
Warp occupancy	12.5%	10.0%	14.1%

**Table 1.** Scaling trends of the compute capabilities of NVIDIA datacenter GPUs across generations, and their occupancy characterization of CUTLASS GEMM kernels.

memory and barrier synchronization [19]. The clustered organization of cores enables more number of threads to share data through such hardware primitives.

Specifically, GEMM kernels on GPUs make extensive use of the shared memory to maximize data reuse in the on-chip memory. With modern workloads like large language models (LLMs) requiring increasingly large GEMM operations, there is a growing need for improved data reuse and communication at the cluster level. This necessity motivates the rationale for integrating matrix units at the cluster level, a key principle that guides the development of the Virgo system.

### 2.2 State-of-the-art Tensor Core Integration

To meet the rapidly increasing compute demand of deep learning applications, NVIDIA introduced dedicated matrix units known as *Tensor Cores* in the Volta architecture [8]. Tensor Core consists of multiple SIMD-parallel dot product units designed for high-throughput multiply-add operations across SIMD lanes [31]. As shown in Figure 1(a), Tensor Cores receive matrix operands directly through the register file of the SIMT core, similar to other execution units such as CUDA cores and the load/store unit. Essentially, today’s Tensor Core is a specialized execution unit that is tightly coupled into the execution pipeline of the SIMT core. Prior efforts have focused on improving the Tensor Core design in sparsity support [17, 22, 41] and generalized operations [37, 44], while maintaining the core-coupled integration.

Notably, Tensor Core has been rapidly increasing in its compute capabilities. Table 1 outlines the evolution of NVIDIA datacenter GPUs across generations [8, 9, 11]. The FP16 throughput of Tensor Cores has improved at a rate surpassing that of FP32 throughput in CUDA cores. This increase in compute throughput is not due to an increase in the number of Tensor Cores, but rather to each Tensor Core instance growing larger in size. This trend underscores the need to scale up Tensor Core capabilities for future generations of GPUs.

### 2.3 Limitations of the Core-Coupled Approach

However, the tightly core-coupled nature of today’s Tensor Core design poses significant challenges to further scaling of the matrix unit. First, modern GEMM kernels, which are increasing in size, generate high *register pressure* as they require extensive use of register file space to store multiple input and accumulator tiles [25]. This issue is compounded in matrix units, where input matrix tiles must be entirely stored within the register file, significantly increasing the register usage. As a result, this leads to decreased kernel occupancy or frequent register spills to stack memory in Tensor Core-accelerated GEMM kernels, as reported in previous studies [4, 38, 40, 42, 43]. Our characterization of CUTLASS confirms this, where the average register use per thread across its GEMM kernel variants is very high, leading to low occupancy (Table 1). While low occupancy does not directly lead to lower performance, it underlines the challenge in further scaling up the size of matrix units given the current capacity constraints. Efforts like INTERPRET [27] and Duplo [26] are developed to reduce duplicated data in the register file, alleviating capacity constraints.

Furthermore, the tight coupling to the SIMT core’s register file imposes not only *capacity* constraints, but also *bandwidth* constraints. According to [31], the register read bandwidth available in the Volta architecture is maximally utilized during Tensor Core operations. To scale up the operation size, an increase in register file bandwidth is necessary to accommodate the larger operand data to the Tensor Core, posing significant design challenges.

Due to register file constraints, core-coupled matrix unit designs typically support *fine-grained* operations. For example, the NVIDIA Tensor Cores handle tile sizes of  $16 \times 8 \times 16$  for FP16 input operands in the `mma` instruction [12]; similarly, AMD CDNA2 Matrix Cores supports sizes of  $16 \times 16 \times 16$  and  $32 \times 32 \times 8$  in the MFMA instruction [33]. These small tile sizes require processing a large number of instructions to complete the entire GEMM operation. This results in significant energy and power consumptions in hardware components beyond the matrix unit itself, such as register file, instruction issuing, and the warp scheduling logic.

### 2.4 Recent Advances and Remaining Challenges

The Hopper Tensor Core, released in 2022, addresses register pressure by introducing the new `wgmma` instruction, which can read matrix operands directly from shared memory, reducing reliance on the register file [11, 29], while keeping the Tensor Core tightly coupled to the SIMT core. This new operand delivery method mitigates the need to store the matrix data in the register file, alleviating the scalability limitation, as evidenced by the significant increase of MACs per Tensor Core in Hopper shown in Table 1.

However, the Hopper Tensor Core does not fully solve the register pressure issue, and energy efficiency remains a

concern. The `wgmma` instruction, while reducing some register load, still requires writing the result matrix back to the register file [12], generating significant register pressure. Additionally, the Tensor Core is still tightly coupled to each SIMT core [11, 29], preventing data sharing between units. This limitation restricts data reuse compared to a large unified design, reducing achieved energy efficiency.

Virgo fundamentally address the scalability and energy efficiency challenges by completely disaggregating the matrix unit from the SIMT cores, establishing it as a separate instance at the cluster level. To the best of our knowledge, Virgo is the first to integrate a matrix engine at this level. Virgo’s matrix unit, drawing operand directly from shared memory, bypasses the core’s register file completely, eliminating the capacity and bandwidth constraints. Moreover, because the hardware can operate on larger matrix operands, the granularity of operation increases, reducing the number of instructions in the pipeline, and thereby cutting down on power and energy consumption. Next, we will detail the Virgo microarchitecture (Section 3) and its programming model (Section 4).

## 3 Virgo Microarchitecture

Virgo aims to improve scalability and energy efficiency by disaggregating the dedicated matrix unit from the core as a separate hardware at the cluster level. To realize this design, we need to solve several microarchitectural challenges: (1) establishing a command interface through which the core and the unit can communicate, (2) designing a cluster-local shared memory interconnect that efficiently handles concurrent accesses from the core and the matrix unit, (3) facilitating a more efficient matrix data movement via a dedicated DMA engine. and (4) implementing a synchronization mechanism across the cores and the matrix unit. We discuss these components in more detail in the following subsections.

Before we begin, we mention key open-source hardware infrastructures that we leverage to realize our design at the RTL. First, we use Vortex [39], an open-source GPGPU implementation in SystemVerilog that enables the full stack of both hardware and kernel development by extending the RISC-V ISA. Second, we use Gemmini [18], a Chisel-based systolic array generator, to generate the cluster-based matrix unit IP for Virgo<sup>1</sup>. We describe in further detail how we modify these IPs to establish a full GPU system in Section 5.

### 3.1 Command Interface to the Matrix Unit

We facilitate the cluster-local interconnect to establish an efficient memory-mapped IO-based command interface between the core and the matrix unit. The MMIO interface is advantageous in our design because it does not require modification of the ISA and the core microarchitecture: At the

<sup>1</sup>Utilizing *Vortex* and *Gemmini* to realize cluster-level integration motivates the name *Virgo*.

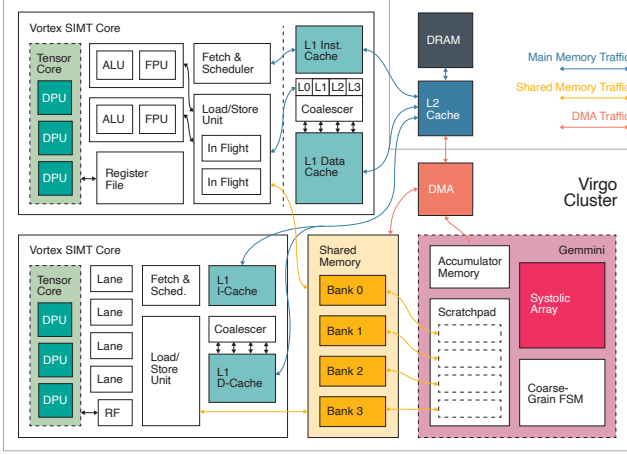


**Figure 2.** Microarchitecture of a Virgo cluster. The Gemini-based matrix unit is disaggregated from the SIMT cores into a separate unit, receiving its operand through the shared memory. Dashed lines indicate optionally instantiated modules for evaluation, such as the core-coupled Tensor Core.

kernel, the core controls the matrix unit simply by issuing regular loads and stores to a specific memory address region. At the same time, the core still benefits from low-latency access to the memory-mapped registers that are interconnected to the lightweight, cluster-local NoC.

Since the Gemini-generated matrix unit IP only supports the RoCC interface [3], we replace the interface with registers mapped to the shared memory address space. To support explicitly synchronizing with Gemini, we replaced the previously used RISC-V fence instruction with a fast routine polling Gemini’s busy status, mapped to an address. When performing GEMM, a hardware FSM exists in Gemini to automatically iterate through the  $i$ ,  $j$  and  $k$  dimensions, allowing a single invocation to fully compute on matrix sizes larger than the systolic array dimensions. The FSM retrieves operands from the shared memory, controls systolic array operation, and writes the result matrix to the accumulator memory. We discovered that the Gemini utilization was frequently bottlenecked by the low instruction throughput from the Vortex cores; to remedy this, we implemented further coarser-grained instructions at the FSM to enable the cores to fully utilize Gemini operations using fewer instructions.

### 3.2 Memory System

The main challenges of Virgo’s memory system involves handling concurrent, heterogeneous accesses to the shared memory from both the core and the matrix unit, and achieving high effective bandwidth in fetching matrix data from the global memory. The following subsections discuss each of these challenges.

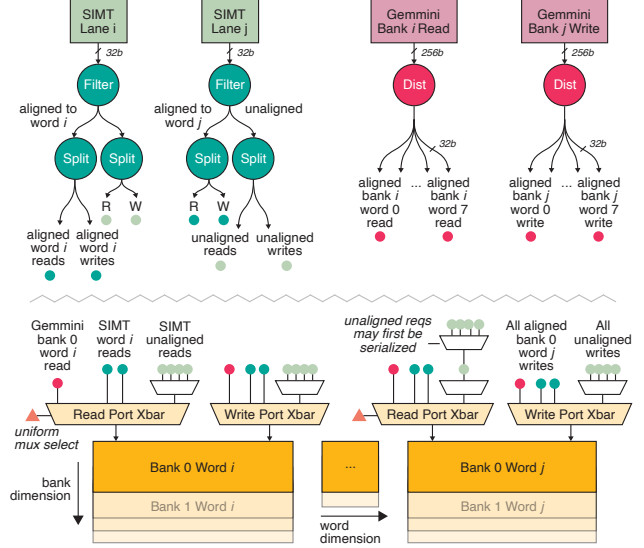


**Figure 3.** The Virgo shared memory system. The SIMT requests go through nodes to maximize aligned throughput while minimizing area overhead; wide matrix unit accesses are broken down to mix with SIMT requests.

**3.2.1 Shared memory and interconnect.** The shared memory system needs to be able to handle several challenges. First of all, the SIMT cores and the matrix unit have different shared memory traffic patterns which when issued concurrently leads to bank conflicts. Specifically, the SIMT lanes of a Vortex core issues 32-bit word-sized memory accesses, while the Gemini-based Virgo matrix unit makes much wider accesses to feed the  $n \times n$  systolic array. In addition to the width difference, the core and the matrix unit frequently perform opposite read and write operations, especially when they operate in a software-pipelined producer-consumer relationship as will be discussed in Section 4.3.2. Finally, the memory system must be flexible enough to allow scalability in the accelerators, towards a many number of matrix units or even towards a heterogeneous different-sized configuration, which we will evaluate in Section 6.1.

To tackle these challenges, we make the following key design choices, depicted in Figure 3:

- *Two-dimensional banking.* To accommodate the aforementioned different-sized accesses from the core and matrix units while incurring minimal bank conflicts, we partition shared memory address space in two dimensions: banks and words. This allows parallelism for memory accesses arriving at different words, or different banks.
- *Unified request sizes.* We *distribute* the wide Gemini requests into the same word-sized sub-requests as the SIMT cores, served in the same cycle to emulate access to a wide bank. This allows the smaller SRAM banks to still have the flexibility to serve smaller individual

requests, while wide requests are served with minimal behavior changes. The muxes use the same mux select across all words in a bank, while prioritizing the wider requests over the narrow word-sized requests. This ensures Gemmini’s wide requests are served in the same cycle, allowing it to operate at full throughput.

- *Separate read and write paths.* The SIMT requests uses the same channel for reads and write; these channels are demuxed into separate channels for each operation. From that point forward, the read and write connection graphs become disjoint, i.e. no channels serve both types of requests. On the opposite direction, read and write responses are muxed back into the SIMT cores. This better supports the aforementioned producer-consumer relationship scenarios.
- *Area optimization for unaligned SIMT accesses.* We find that connecting every SIMT core’s memory access lanes to every SRAM modules via a crossbar results in prohibitive area cost. To remedy this, we implement *Filter* nodes that selectively filter out word-aligned core memory requests into a channel that is directly wired to the SRAM banks, while serializing unaligned requests in a separate channel. We find this optimization makes minimal impact to the evaluated kernels, as the kernels frequently make word-aligned access to the shared memory for moving matrix data.

We make extensive use of TileLink [7] and Diplomacy [35] which enables a highly parameterized implementation of the memory interface for different numbers of cores, matrix units, and memory widths in the cluster.

**3.2.2 Memory coalescer.** GPU’s memory system is optimized for throughput, and it is crucial to efficiently utilize wide vectorized loads and stores available in the system to achieve high *effective* memory throughput and thereby overall performance. At the onset of the project, Vortex had lacked hardware support for merging adjacent SIMD scalar memory accesses into wider accesses, also known as *memory coalescing* [14]. To remedy this, we implemented a custom memory coalescing unit at the interface between the core and the L1 cache, as shown in Figure 2. The coalescer monitors the global memory accesses made by the core’s SIMD lanes, and if possible, merges them into wider memory requests that are of the L1 cache line size. The incorporation of the coalescer significantly improved the rate of data delivery from the global memory (i.e. L2 and L1 cache) to the core, and facilitated in achieving realistic memory bandwidth.

### 3.3 Efficient Data Movement with DMA

To keep the matrix units fed with valid operands, the memory system needs to be able to move the matrix tile data across different levels in the memory hierarchy efficiently: the shared memory, the global memory (L1/L2/DRAM), and the matrix unit’s private accumulator memory. We find that

using regular loads and stores in the SIMT core for moving matrix data from global to shared memory significantly limits the matrix unit utilization (Table 3), due to both address computation overhead and low instruction throughput of the Vortex core. We therefore incorporated a programmable DMA engine to efficiently move the matrix tile data across the memory hierarchy and achieve higher operand delivery bandwidth to the matrix unit. As shown in Figure 2, data can be transferred in all but one direction in the combinations between L2, the shared memory and the matrix unit accumulator memory. The matrix shape, size and transpose operations of the data movement can be programmed via a separate MMIO-based interface described in Section 3.1

Note that the design of the DMA is not tied to Virgo’s matrix unit; it can also be incorporated to the baseline core-coupled design. We evaluate this configuration as well to model an Ampere-like design that features both the Tensor Core and an asynchronous data copy engine [10]. This allows us to order to better evaluate the effect of our cluster-level integration mechanism in isolation.

### 3.4 Cluster-wide Synchronization

As will be made clear in Section 4, the SIMT cores in a cluster work together collaboratively to move matrix data for the matrix unit, or do post-processing computation on the resulting matrix from the unit. This requires an efficient synchronization mechanism across the cores to be implemented at the entire cluster level. To this end, we design a lightweight synchronizer module instantiated at each cluster that interfaces with the warp scheduler of each SIMT core. When a designated set of warps reach the barrier instruction, the warp scheduler issues a barrier release request to the synchronizer. The synchronizer collects requests from other cores, and replies with a response only when all cores have made a request, making sure every core participates in the barrier. Vortex implements a similar inter-core synchronization mechanism, but only at the device-wide scope that enforces all core’s participation. We reuse Vortex’s `vx_bar` instruction to allow the programmer to specify which warps participate in a particular barrier, and be able to use multiple barriers in the kernel. This is important to enable the programmer to utilize multiple matrix unit instances in a single kernel, as will be shown in Section 6.3.

## 4 Virgo Programming Model

As a result of disaggregation from the core and increased scalability, Virgo’s cluster-level matrix unit operates on larger matrix tiles than the core-coupled designs, which incurs longer latency for a single operation. While SIMT cores in GPUs employ warp multithreading which efficiently hides latency for finer-grained operations of Tensor Cores, it is not sufficient to completely hide the longer operation latency

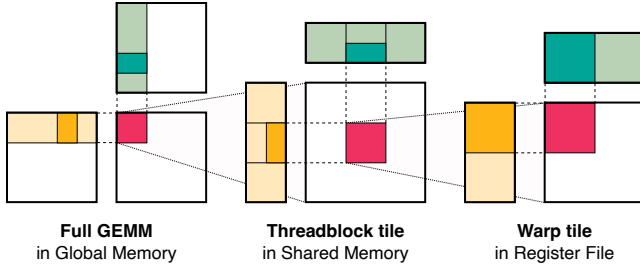


**Figure 4.** Tiled GEMM on GPUs [25]. GPU GEMM kernels employ tiling at multiple levels to leverage data reuse. Tensor Cores accelerate *warp tile* operations using dedicated hardware, while Virgo accelerates *threadblock tile* operations.

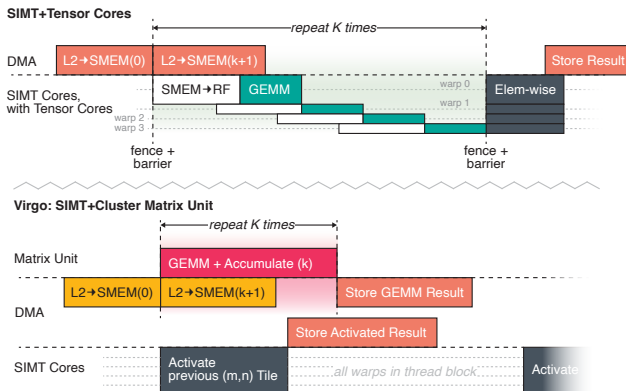


**Figure 5.** Asynchronous execution scheme of the matrix unit and SIMT cores in Virgo during a GEMM operation, compared to the Tensor Core-based design. The loop illustrated here maps to a single threadblock tile in Figure 4.

of Virgo’s matrix unit solely through the existing mechanisms of SIMT. Therefore, Virgo provides an *asynchronous* programming interface to allow the programmer to maximally utilize compute resources in the SIMT core, concurrent to the matrix multiplication operation.

#### 4.1 Asynchronous Programming of Matrix Unit

As discussed in Section 3.1, the Gemini-based matrix unit in Virgo exposes a memory-mapped IO interface to the core. The accesses to the MMIO interface are non-blocking, such that the core can kick off an execution of Gemini and then proceed to execute the next instructions in the kernel. Specifically, since MMIO interface does not require parallel accesses from multiple SIMT threads, the kernel is written in a way to elect a singular thread that is responsible for issuing loads and stores to the MMIO using a divergent branch. After kicking off Gemini, the core can then execute independent operations such as data movement for the next tile or post-processed activation on the previous one, as will be detailed in Section 4.3.

Virgo also allows for instantiating multiple Gemini units at each cluster, in which case Virgo establishes separate multiple MMIO interfaces at disjoint address regions per unit. Each unit has a unique cluster-local ID that the programmer can use as a handle. Using this mechanism, the programmer fully manages how to partition work onto the different Gemini units.

#### 4.2 Collaborative Execution of Warps

GEMM operation on GPUs require close coordination between the threads in the SIMT core and the dedicated matrix unit, where the threads may handle data movement between the off-chip and on-chip memory, or post-processing compute on the result matrix such as non-linear activations in a deep learning workload. Because the matrix unit operates on a larger tile size in Virgo than in core-coupled designs, *multiple* warps collaborate to participate in a *single* matrix unit operation, to achieve adequate throughput matching. This is depicted in Figure 5, where all warps in the thread block participate in activating the previous  $(M,N)$  output tile computed by the matrix unit operation. The collaborative execution of warps requires the cluster-wide synchronization mechanism described in Section 3.4, because the warps in the thread block may be running in different cores in the cluster.

#### 4.3 Mapping to the GEMM Kernel

We now describe how the the aforementioned mechanisms aid the programmer to write an optimized GEMM kernel.

**4.3.1 Thread block tiling.** Virgo builds upon the well-established work partitioning scheme of GEMM kernels on GPUs depicted in Figure 4 [25], where the input matrices are tiled at *multiple* levels to maximize data reuse at the different memory hierarchy. Virgo’s matrix unit accelerates the first level of *thread block* tiling, which leverages parallelism across clusters and caches tiles at the shared memory. In comparison, Tensor Cores accelerate the second level of *warp* tiling, using register file as data storage.

In our configuration, the matrix unit exposes  $64 \times 64 \times 64$  as the tile size of a single operation, which determines the thread block size. Each thread block, spatially partitioned across the  $(M,N)$  output space, completes the full GEMM by accumulating across the  $K$  dimension temporally in a loop, shown in Figure 5. As the loop iterates, the Gemini matrix unit accumulates partial sum data onto its private accumulator memory, which gets moved out and stored to the global memory at the end of the loop.

The thread blocks are *persistent* similar to CUTLASS [25]: Instead of launching a new thread block for every  $(M,N)$  output tile, a single thread block computes multiple outputs in a loop throughout its lifetime. This amortizes the start and teardown runtime overhead that happens at every launch.

**4.3.2 Software pipelining and double buffering.** Importantly, the Virgo-optimized GEMM kernel employs *software pipelining* which is enabled by the asynchronous programming interface of the matrix unit. As shown in Figure 5, while the matrix unit is computing a tile along the K dimension consisting a *consumer* pipeline, either the DMA unit or a set of SIMT core warps collaboratively fetch the next input tile along the K dimension from the global memory to the shared memory, consisting the *producer* pipeline. Another set of SIMT core warps can collaborate to form an additional consumer pipe that does post-processing activation compute on a previous result tile. Because both the producer and consumer pipes run in parallel, the tile data are double-buffered in the shared memory. This mechanism allows both the SIMT core warps and the matrix unit to participate in useful work at all times, maximizing utilization of all hardware components in the cluster.

#### 4.4 Comparison to Programming Tensor Cores

The key difference in the programming model for Tensor Core is that the operations are *synchronous*. As depicted in Figure 5, the warp simply stalls execution until the Tensor Core instruction finishes writing back the result to the register file, where the data dependency is handled by the hardware and is implicit at the kernel code. On the contrary, in Virgo’s asynchronous programming model, the data dependency between SIMT warp execution and the matrix unit execution is explicitly managed by the programmer using software synchronization primitives and fences.

## 5 Methodology

We leverage and extensively modify key infrastructure components such as Vortex and Gemini to enable our full system design at the RTL level. In this section, we outline the modifications we make to the different SoC components in detail, and then set up experiments for evaluation.

### 5.1 System Implementation

We use the Chipyard SoC generator framework [2] to integrate all hardware components into a single SoC design: Vortex SIMT cores, matrix units, shared memory, cache, and on-chip interconnects. In addition, the Chipyard SoC is highly parameterizable, in terms of the number of cores and clusters, the processing element dimensions in the matrix unit, memory system parameters, data types, and more. This allows Virgo to be a flexible and comprehensive generator covering a large design space.

**Vortex SIMT Cores.** We adapted the SIMT core and L1 cache modules from Vortex (VX\_core and VX\_cache) to construct our own cluster hierarchy and synchronization mechanisms, rather than incorporating the full top-level design. We pass the global memory traffic from Vortex through our coalescer, before reaching the Vortex cache bank based L1

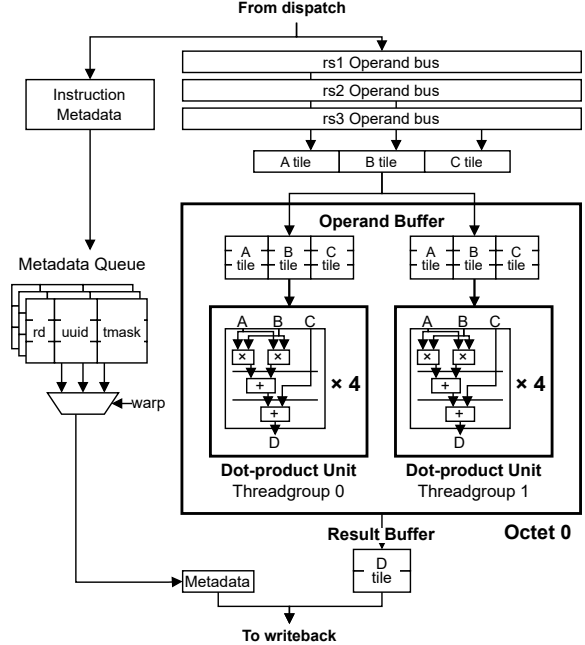


**Figure 6.** Microarchitecture of the Volta Tensor Core [31] as implemented in Virgo’s RTL, evaluated as the baseline core-coupled matrix unit design.

caches. In addition to inserting Tensor Cores to its pipeline, we made numerous modifications to the Vortex core RTL to facilitate higher IPC and memory throughput. The modifications include adding support for memory store fences, optimizing the warp scheduling logic, and implementing cluster-level synchronization primitives. In practice, we found these changes resulted in better performance for non-matrix-unit operations and allowed us to better focus on challenges that pertain to the different integration methods of the matrix unit.

**Gemini.** We make extensive modifications to Gemini in order to make the systolic array directly interface with the cluster-level shared memory. Gemini coordinates the movement of the source matrices from its private wide scratchpad banks through its systolic array, accumulating at either the individual processing elements or at its private accumulator memory, depending on the selected dataflow. For Virgo, we retained the accumulator memory to ensure full systolic array throughput, which required single-cycle accumulation. We modified the scratchpad interface to use the TileLink protocol and go through the SMEM interconnect, instead of directly interfacing with SRAMs. The SIMT cores can therefore deposit data into the SMEM directly for Gemini to process.

**Tensor Cores.** To faithfully model the baseline GPU with core-coupled matrix units, we closely implement in RTL the microarchitecture of Volta Tensor Core proposed in [31],

whose timing behavior is well correlated to the NVIDIA GPU.

Figure 6 shows the detailed microarchitecture of the Tensor Core module as implemented in the RTL. It mainly consists of SIMD-parallel dot-product units that execute multiply-and-accumulate operations with tree reductions on the input tile fragments. As a result of tight coupling to the core, the tile fragments are directly supplied by the register file.

Because Vortex cores have different design parameters from Volta, we need to appropriately scale the Tensor Core to achieve full efficiency of the hardware. First, to address the difference in SIMD width (8 in Vortex vs. 32 in Volta), we instantiate a single octet instance instead of four in the original design [31]. Second, we scale the tile size to accommodate the lower operand throughput available for Vortex. Since the Vortex core does not provide native support for FP16 operands in the ISA, the matrix data type is limited to FP32, effectively halving the available operand throughput for Vortex. We address this by halving the K dimension of the input tiles. As a result, the tile size of a single  $wmma$  instruction becomes  $(m, n, k) = (8, 8, 8)$ , scaled down from  $(16, 16, 16)$  in Volta.

Through microbenchmarks, we verify that our Tensor Core implementation achieves identical timing behavior of 2 cycles per operation as in Volta, with identical compute throughput of 512bits ( $4 \times 4 \times 2$  FP16 in Volta,  $4 \times 2 \times 2$  FP32 in Vortex) per octet per cycle. Both Tensor Core and Gemini use the same HardFloat [20] implementation for floating point units to facilitate fair area and power comparison.

## 5.2 Experiments

In this subsection, we will detail the environment in which the workloads are run, the specifics of the kernels, as well as the tools we use to run them.

**Hardware Setup.** We summarize in Table 2 the hardware configuration of the two GPU designs we evaluate comparatively: the core-coupled design and Virgo. Note that only the GPU SoC parameters are common to both designs. Both the Tensor Core and Virgo matrix unit uses *hardfloat* [20] floating point modules to implement the MAC units, each fully pipelined to 1 operation per cycle. Virgo matrix unit is sized in such a configuration so that both types of the matrix unit provisions the same number of MACs per cluster for a fair comparison.

**Workloads.** We implement GEMM kernels independently optimized for Virgo and core-coupled designs, with different dimensions:  $256 \times 256 \times 256$  (*small*),  $128 \times 512 \times 512$  (*medium*), and  $512 \times 512 \times 512$  (*large*). Each matrix multiplication kernel is run on the Virgo design as well as the core-coupled design, with and without incorporating DMA, resulting in four configurations per kernel. We write the kernels in C and use Vortex’s LLVM compiler toolchain to generate binaries.

To demonstrate how the SIMT core’s compute resource freed up by the larger operation granularity of cluster-level

GPU SoC Configuration	
Clusters	1
Cores per cluster	4
SIMT Width	8 warps/core, 8 lanes/warp
SIMD Units	2 ALUs, 1 FPU, 32 LSQ entries per lane
Issue Width	8 warps
Register File	64 KB
Shared Memory	64 KB, 4 banks, 8 sub-banks
L1 Cache	16 KB instruction, 16 KB data per core
L2 Cache	512 KB
Tensor Core Configuration	
Tensor Cores	1 per core (4 per cluster)
FP32 MACs	16 (64 per cluster)
Virgo Configuration	
Matrix Unit	1 per cluster
Systolic Array	$8 \times 8$
FP32 MACs	64
Accumulator Memory	16KB

**Table 2.** Hardware configuration of the GPU designs used for evaluation.

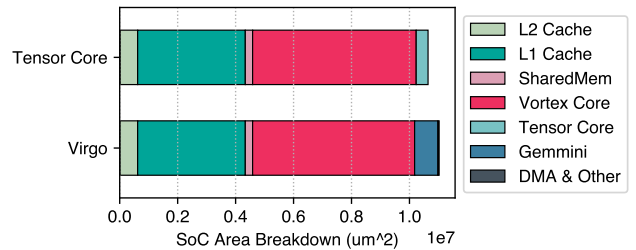


**Figure 7.** Area breakdown by SoC components. The Virgo-based design has 3.6% larger area than the core-coupled Tensor Core-based design.

matrix unit can be utilized for useful work other than GEMM, we implement a simple fused kernel that runs both GEMM and a non-linear Swish activation [32] in a software-pipelined manner, both Virgo and on core-coupled designs.

In addition, to further demonstrate the scalability and flexibility of the matrix unit integration system consisting of the interconnect, command interface, and synchronization primitives, we also create a heterogeneous hardware configuration with two differently sized matrix units in the same cluster: an  $8 \times 8$  unit and a  $4 \times 4$  unit. We show the utilization results of a kernel that concurrently schedules two differently-sized matrix multiplications on both units.

**Tools & Measurement.** We synthesize the design at 400 MHz using a commercial 16 nanometer process. We use Cadence Joules to estimate power, and use Cadence Genus to estimate area, as well as verify the operating frequency. An area breakdown of the synthesized SoC design configured



to Table 2 is shown in Figure 7. The Virgo design has 3.6% larger SoC area than the core-coupled design. The L1 cache consumes a large area as it is synthesized as flop arrays rather than SRAMs; however, we do not find this affects the key findings in our evaluation. Additionally, we used FireSim [24] to verify the design to be functional on a Xilinx Alveo U250 FPGA.

For all power and energy evaluation in the subsequent sections, we plot and discuss *active power*. This measure is obtained by taking the nominal SoC-wide power, and subtracting the SoC power at an idle state where the cores do not retire any instruction. We find this is necessary to provide a meaningful comparison between Virgo and the core-coupled design, as otherwise the power consumption in the core alone is extremely high even at the idle state, possibly due to the absence of clock gating and high switching activities. Discussing active power allows us to distinguish the more generalizable power implications that arise from our design choices, from those that depend on a specific implementation.

## 6 Evaluation

### 6.1 GEMM Kernels

We first evaluate execution of GEMM kernels on both the cluster-level Virgo design and the core-coupled Tensor Core design. The kernels are written separately for the Virgo and core-coupled design with bespoke optimizations, including double-buffering, warp specialization and persistent threads [25].

Overall, Virgo achieves higher MAC utilization across all GEMM configurations due to its larger operation granularity alleviating constraints from the instruction throughput from the core. Virgo is also up to 66.3% more active power efficient and 77.2% active energy efficient than the core-coupled design, with the most major source of power reduction being the core due to the reduced instruction processing.

**6.1.1 Performance and utilization.** Table 3 lists the cycle count and utilization figures for the three GEMM sizes, run under numerous hardware configurations. Utilization is calculated by dividing the ideal number of cycles driven from the GEMM dimensions and the number of MAC units in the hardware, by the actual number of cycles taken in the simulation. As shown in the table, the cluster-level matrix unit in Virgo shows a large increase in MAC utilization compared to the core-coupled Tensor Cores, both with and without DMA. The Virgo matrix unit achieves high utilization numbers across all GEMMs, including a non-square-shaped configuration; with the largest GEMM size, Virgo is able to achieve 91.0% utilization, close to the theoretical maximum.

The Virgo matrix unit is able to achieve higher utilization mainly because the core asynchronously offloads a larger body of compute to the matrix unit per operation, whereas core-coupled matrix units need to be driven by

	256×256×256		128×512×512		512×512×512	
	Cyc.	%Util	Cyc.	%Util	Cyc.	%Util
TC	726k	36.1	1450k	36.2	5.79M	36.2
TC + DMA	458k	57.2	832k	63.0	3.34M	62.7
Virgo	540k	48.5	941k	55.7	3.71M	56.5
<b>Virgo + DMA</b>	<b>310k</b>	<b>84.5</b>	<b>583k</b>	<b>90.0</b>	<b>2.30M</b>	<b>91.0</b>

**Table 3.** Execution cycle time and % utilization of the MAC units in Virgo and baseline core-coupled Tensor Core (“TC”) designs for running GEMM kernels of three different sizes.

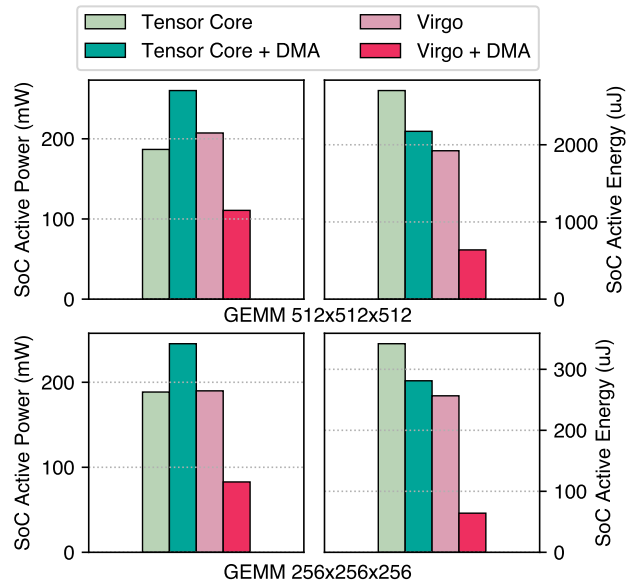


**Figure 8.** Active power and energy comparison between Virgo and the baseline Tensor Core design, with and without incorporation of DMA.

finer-grained instructions with smaller tile sizes. Therefore, the core-coupled unit requires the core to process more instructions for a given GEMM size, and its utilization is thus constrained by the instruction issue rate of the core. We note that our utilizations that we achieve for the core-coupled design is in line with that in other works [15, 42].

For both Virgo and core-coupled designs, DMA appears to be critical for high utilization. Without DMA, the kernel relies on load/store instructions for data delivery where the instruction issue rate becomes the limit. Moreover, the core is responsible for generating memory addresses with integer instructions, further decreasing the achieved memory throughput. This results in matrix units being starved for operand data.

**6.1.2 Power and energy.** In Figure 8 we show a side-by-side comparison between the power usage of Virgo and core-coupled Tensor Core based designs. Comparing both designs

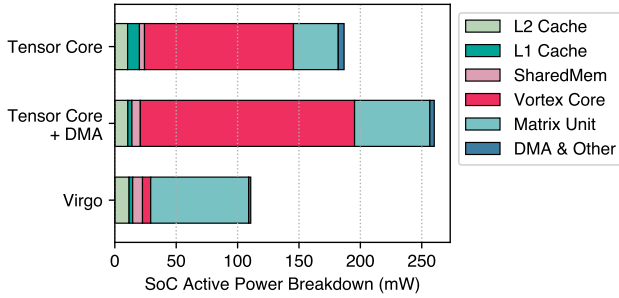


**Figure 9.** Active power breakdown by SoC components. The core active power is reduced significantly as a result of reduced instruction processing in Virgo. Matrix unit power is higher in Virgo due to higher MAC utilization.

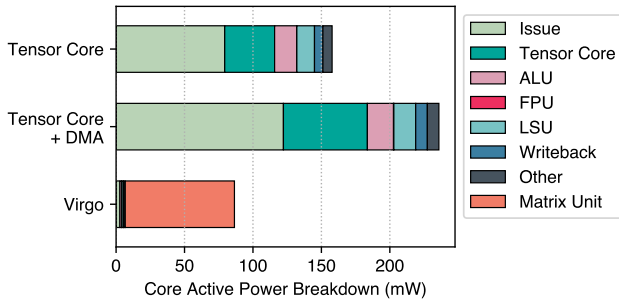


**Figure 10.** Active power breakdown of the Vortex SIMT core for the  $512 \times 512 \times 512$  GEMM kernel. Note that although the Gemmini-generated matrix unit resides outside the core in Virgo, we add its power consumption for better comparison.

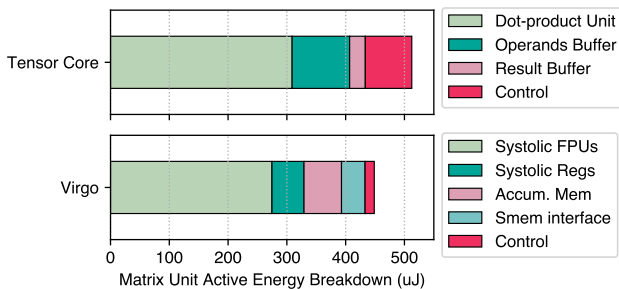


**Figure 11.** Active energy breakdown of the matrix unit for the  $512 \times 512 \times 512$  GEMM kernel.

with DMA, Virgo reduces active power by up to 66.3% in the *large* kernel. Combined with higher utilization of the matrix unit, active energy reduction is even higher, at 70.7%. The *medium* kernel exhibits similar power characteristics to the *large* and *small* kernels shown in the figure.

To better reason about the source of power consumption in the hardware, we give a detailed power breakdown at the SoC (Figure 9), the SIMT core (Figure 10), and the matrix

units (Figure 11). Importantly, comparing Virgo to Tensor Core designs shows most of the reduction in power occurs in the core, instead of the matrix units themselves.

**Larger operation granularity reduces core power.** Figure 10 gives a more detailed power breakdown across the pipeline stages inside the SIMT core. Notably, the majority of the core power is consumed in the issue stage. The issue stage is responsible for dynamically tracking data dependencies and scheduling warps, as well as handling read and write accesses to the register file. Because the core-coupled Tensor Core has a much *finer operation granularity*, it requires processing a large number of instructions in the issue stage, which causes higher power consumption.

On the contrary, Virgo achieves a significantly lower overall power consumption by *coarsening* the granularity of operation and reducing the incidental power consumption outside the matrix unit proper. Measuring pipeline activity of the core confirms this observation: In Virgo, the number of retired instructions is 8.17% of that of the Tensor Core design. In terms of the register accesses, Virgo does 4.57% of the read and write accesses to the register file that the core-coupled design does.

**Higher utilization compounds to energy efficiency.** The higher utilization of the MAC units that Virgo facilitates by eliminating constraints from the core, compounds with the aforementioned power efficiency to lead to a greater system-level energy efficiency. The total amount of active SoC energy used by both designs, as computed by multiplying power with kernel runtime, is 77.2% less for the *small* GEMM and 70.7% less for the *large* GEMM in Virgo.

**Matrix unit energy savings.** Figure 11 shows a detailed breakdown of energy consumption inside the matrix units. Although the two designs consume similar amounts of energy in the floating-point units, Virgo uses less energy in its registers. We find that Tensor Core requires use of FIFO queues with sufficient depth to buffer the matrix data and absorb backpressure from the core pipeline in order to perform well. Combined with the control logic to manage the buffers and dot-product unit stalls, the in-unit energy is higher. Moreover, Virgo’s matrix unit is a systolic array design that is unified at the cluster level, unlike Tensor Cores which are distributed across the SIMT cores. This enables Virgo to facilitate better data reuse and do fewer accesses to its flop registers, reducing energy consumption. Some of these advantages are offsetted by the use of a sophisticated sharedmem interface and the private accumulator memory.

However, we note that the energy reduction in the SIMT cores that we discussed earlier plays a much greater role in the full system context, than that in the matrix units. The choice of systolic array for the matrix unit is not crucial to achieving Virgo’s energy efficiency.

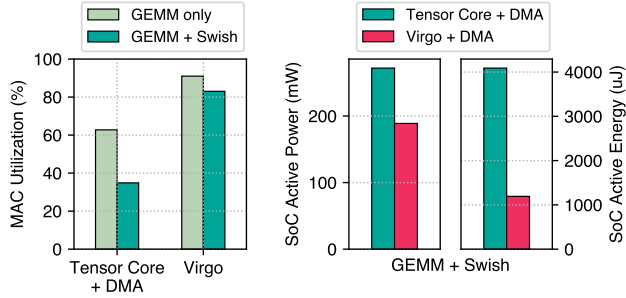


**Figure 12.** Left: MAC utilization for the fused GEMM and Swish activation kernel, compared to the GEMM-only kernel. Right: Power and energy of the fused kernel. Virgo’s minimal utilization loss shows that it better repurposes the SIMT compute resources for non-GEMM operations.

## 6.2 Concurrent Matrix Unit and Core Execution

Modern machine learning workloads increasingly rely on fused GEMM and non-linear activation kernels to minimize off-chip memory accesses [13, 16]. Virgo’s decoupled architecture opens up new opportunities for a more efficient mapping of fused kernels through concurrent execution of the GEMM operation in the matrix unit, and non-GEMM operations in the SIMT core.

**Performance and utilization.** Figure 12 shows the MAC utilization of the matrix units in both Virgo and core-coupled designs when executing a kernel that fuses both  $512 \times 512$  GEMM and the Swish activation [32]. While Tensor Cores experience 44.4% degradation in utilization compared to the GEMM-only kernel, the degradation in Virgo is only 8.8%. The minimal degradation in utilization shows that Virgo can better support highly fused kernels used in modern deep learning workloads, while maintaining high utilization in both the SIMD compute units and the matrix unit.

There are two main reasons as to why Virgo allows better concurrent operation of the two compute resources. First, matrix operations are offloaded from the core at a coarser granularity, requiring fewer instruction issues for the same amount of matrix compute. This leaves more issue slots in the core to be used for non-matrix SIMD operations in the activation computation.

Second, the Virgo matrix unit executes asynchronously, which allows concurrent operations to happen within a *single* warp, not only by multithreading across different warps. After issuing a matrix unit operation, the warp can then proceed to execute subsequent non-matrix instructions without stalling. In contrast, Tensor Core instructions are synchronous, necessitating use of warp specialization to schedule both matrix and non-matrix operations concurrently. This results in fewer number of warps being allocated to execute each operation, which leads to suboptimal latency hiding and subsequently lower hardware utilization.

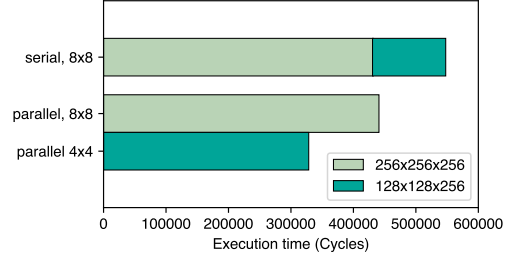


**Figure 13.** Execution time for the multi-Gemmini configuration in Virgo. The *parallel* bars indicate that the two Gemmini instances are capable of running different GEMM operations in parallel to achieve speedup over the single instance case, showing scalability of the design.

**Power and energy.** The minimal degradation in hardware utilization for Virgo leads to better energy efficiency; Virgo’s active SoC energy consumption is 70.8% lower than the core-coupled design (Figure 12).

## 6.3 Multiple Heterogeneous Matrix Units

The clear architectural disaggregation of the matrix unit at the cluster level enables a new design space in Virgo at a low design effort, where *multiple* matrix units with different size configurations are integrated to the cluster. Specifically, the shared memory system described in Section 3.2.1 is designed to be able to scale to multiple agents. Not only the hardware, Virgo’s programming interface is also sufficiently flexible to enable writing a kernel that executes multiple GEMM operations at the cluster in parallel, through an ID-based mechanism described in Section 4.1.

We demonstrate this by instantiating two differently sized matrix units, and evaluating a kernel that executes two matrix multiplications on the two units:  $256 \times 256 \times 256$  large GEMM, and a  $128 \times 128 \times 256$  small GEMM. We run in parallel the large GEMM on the larger matrix unit with  $8 \times 8$  systolic array, and the small GEMM on the smaller  $4 \times 4$  unit. For comparison, we also evaluate a separate kernel that executes the two GEMMs in serial, on a single large  $8 \times 8$  unit.

**Performance and utilization.** Figure 13 visualizes the utilization of the both serial and parallel kernels. In the parallel case, the overall hardware utilization is determined by whichever matrix unit runs for a longer time. The serial and the parallel kernel achieves 59.7% and 59.5% utilization respectively. The fact that the hardware utilization remains nearly constant for the parallel kernel indicates that Virgo cluster’s shared memory and interconnect scales well when adding more compute to the system, demonstrating scalability of Virgo’s design.

**Power and energy.** Compared to a single unit, two-unit design increases active power by 30.4%, slightly higher than the 25% FLOP increase. Active energy increases by 4.7%. The slight decrease in energy efficiency is expected due to the

smaller systolic array having less data reuse, and also the power consumption in the memory interface possibly scaling superlinearly to the number of total MACs.

## 7 Conclusion

In this work, we present *Virgo*, a novel GPU architecture that integrates matrix units at the cluster level. Virgo solves the scalability and energy efficiency challenges faced by core-coupled matrix unit designs in current GPUs by physically disaggregating the matrix unit hardware from the core microarchitecture into a separate unit interconnected at the cluster. This disaggregation obviates the need to deliver operand data solely from the register file, eliminating capacity and bandwidth constraints. As a result, we can instantiate the cluster-level matrix unit with a larger operation size than what is possible with core-coupled designs. The resulting larger granularity of operation not only enables better data reuse, but also reduces the number of instructions processed in the core, minimizing incidental energy expenditure and improving overall system-level energy efficiency.

We implement our design using synthesizable RTL and evaluate with GEMM kernels, which shows significant improvement in power and energy efficiency. Furthermore, we demonstrate that the architectural decoupling in Virgo further allows efficient concurrent and collaborative execution between the matrix unit and the SIMT core, or integrating multiple matrix units of heterogeneous configuration, enabling new strategies for mapping applications to the design.

## References

- [1] AMD. Amd cdna 2 architecture. <https://www.amd.com/content/dam/amd/en/documents/instinct-business-docs/white-papers/amd-cdna2-white-paper.pdf>, 2021.
- [2] Alon Amid, David Biancolin, Abraham Gonzalez, Daniel Grubb, Sagar Karandikar, Harrison Liew, Albert Magyar, Howard Mao, Albert Ou, Nathan Pemberton, et al. Chipyard: Integrated design, simulation, and implementation framework for custom socs. *IEEE Micro*, 40(4):10–21, 2020.
- [3] Krste Asanovic, Rimas Avizienis, Jonathan Bachrach, Scott Beamer, David Biancolin, Christopher Celio, Henry Cook, Daniel Dabbelt, John Hauser, Adam Izraelevitz, et al. The rocket chip generator. *ECS Department, University of California, Berkeley, Tech. Rep. UCB/ECS-2016-17*, 4:6–2, 2016.
- [4] Ganesh Bikshandi and Jay Shah. A case study in cuda kernel fusion: Implementing flashattention-2 on nvidia hopper architecture using the cutlass library. *arXiv preprint arXiv:2312.11918*, 2023.
- [5] Robert A Bridges, Neena Imam, and Tiffany M Mintz. Understanding gpu power: A survey of profiling, modeling, and simulation methods. *ACM Computing Surveys (CSUR)*, 49(3):1–27, 2016.
- [6] Tom Brown, Benjamin Mann, Nick Ryder, Melanie Subbiah, Jared D Kaplan, Prfulla Dhariwal, Arvind Neelakantan, Pranav Shyam, Girish Sastry, Amanda Askell, et al. Language models are few-shot learners. *Advances in neural information processing systems*, 33:1877–1901, 2020.
- [7] Henry Cook. *Productive Design of Extensible On-Chip Memory Hierarchies*. PhD thesis, ECS Department, University of California, Berkeley, May 2016.
- [8] NVIDIA Corporation. Nvidia tesla v100 gpu architecture. <https://images.nvidia.com/content/volta-architecture/pdf/volta-architecture-whitepaper.pdf>, 2017.
- [9] NVIDIA Corporation. Nvidia a100 tensor core gpu datasheet. <https://www.nvidia.com/content/dam/en-zz/Solutions/Data-Center/a100/pdf/nvidia-a100-datasheet-nvidia-us-2188504-web.pdf>, 2022.
- [10] NVIDIA Corporation. Nvidia ampere gpu architecture tuning guide. [https://docs.nvidia.com/cuda/pdf/Ampere\\_Tuning\\_Guide.pdf](https://docs.nvidia.com/cuda/pdf/Ampere_Tuning_Guide.pdf), 2024.
- [11] NVIDIA Corporation. Nvidia h100 tensor core gpu datasheet. <https://resources.nvidia.com/en-us-tensor-core/nvidia-tensor-core-gpu-datasheet>, 2024.
- [12] NVIDIA Corporation. Parallel thread execution isa version 8.5. <https://docs.nvidia.com/cuda/parallel-thread-execution/index.html>, 2024.
- [13] Tri Dao, Daniel Y. Fu, Stefano Ermon, Atri Rudra, and Christopher Ré. Flashattention: Fast and memory-efficient exact attention with io-awareness, 2022.
- [14] Jack W Davidson and Sanjay Jinturkar. Memory access coalescing: A technique for eliminating redundant memory accesses. *Acm Sigplan Notices*, 29(6):186–195, 1994.
- [15] Michael Davies, Ian McDougall, Selvaraj Anandaraj, Deep Machchhar, Rithik Jain, and Karthikeyan Sankaralingam. A journey of a 1,000 kernels begins with a single step: A retrospective of deep learning on gpus. In *Proceedings of the 29th ACM International Conference on Architectural Support for Programming Languages and Operating Systems, Volume 2*, pages 20–36, 2024.
- [16] Roman Dubtsov, Evarist Fomenko, and Babak Hejazi. New cublas 12.0 features and matrix multiplication performance on nvidia hopper gpus, 2023. NVIDIA Technical Blog.
- [17] Ruibo Fan, Wei Wang, and Xiaowen Chu. Dtc-spm: Bridging the gap in accelerating general sparse matrix multiplication with tensor cores. In *Proceedings of the 29th ACM International Conference on Architectural Support for Programming Languages and Operating Systems, Volume 3*, pages 253–267, 2024.
- [18] Hasan Genc, Ameer Haj-Ali, Vighnesh Iyer, Alon Amid, Howard Mao, John Wright, Colin Schmidt, Jerry Zhao, Albert Ou, Max Banister, et al. Gemmini: An agile systolic array generator enabling systematic evaluations of deep-learning architectures. *arXiv preprint arXiv:1911.09925*, 3:25, 2019.
- [19] Guin Gilman, Samuel S Ogden, Tian Guo, and Robert J Walls. Demystifying the placement policies of the nvidia gpu thread block scheduler for concurrent kernels. *ACM SIGMETRICS Performance Evaluation Review*, 48(3):81–88, 2021.
- [20] John Hauser. Berkeley hardfloat. <http://www.jhauser.us/arithmetric/HardFloat.html>, 2019.
- [21] Miro Hodak, Masha Gorkovenko, and Ajay Dholakia. Towards power efficiency in deep learning on data center hardware. In *2019 IEEE International Conference on Big Data (Big Data)*, pages 1814–1820. IEEE, 2019.
- [22] Guyue Huang, Zhengyang Wang, Po-An Tsai, Chen Zhang, Yufei Ding, and Yuan Xie. Rm-stc: Row-merge dataflow inspired gpu sparse tensor core for energy-efficient sparse acceleration. In *Proceedings of the 56th Annual IEEE/ACM International Symposium on Microarchitecture*, pages 338–352, 2023.
- [23] Intel. Introduction to the xe-hpg architecture. <https://www.intel.com/content/www/us/en/developer/articles/technical/introduction-to-the-xe-hpg-architecture.html>, 2022.
- [24] Sagar Karandikar, Howard Mao, Donggyu Kim, David Biancolin, Alon Amid, Dayeol Lee, Nathan Pemberton, Emmanuel Amaro, Colin Schmidt, Aditya Chopra, Qijing Huang, Kyle Kovacs, Borivoje Nikolic, Randy Katz, Jonathan Bachrach, and Krste Asanović. FireSim: FPGA-accelerated cycle-exact scale-out system simulation in the public cloud. In *Proceedings of the 45th Annual International Symposium on Computer Architecture, ISCA '18*, pages 29–42, Piscataway, NJ, USA, 2018. IEEE Press.

- [25] Andrew Kerr, Duane Merrill, Julien Demouth, and John Tran. Cutlass: Fast linear algebra in cuda c++. *NVIDIA Developer Blog*, 2017.
- [26] Hyeonjin Kim, Sungwoo Ahn, Yunho Oh, Bogil Kim, Won Woo Ro, and William J Song. Duplo: Lifting redundant memory accesses of deep neural networks for gpu tensor cores. In *2020 53rd Annual IEEE/ACM International Symposium on Microarchitecture (MICRO)*, pages 725–737. IEEE, 2020.
- [27] Jae Seok Kwak, Myung Kuk Yoon, Ipoom Jeong, Seunghyun Jin, and Won Woo Ro. Interpret: Inter-warp register reuse for gpu tensor core. In *2023 32nd International Conference on Parallel Architectures and Compilation Techniques (PACT)*, pages 309–319. IEEE, 2023.
- [28] Baolin Li, Rohin Arora, Siddharth Samsi, Tirthak Patel, William Arcaud, David Bestor, Chansup Byun, Rohan Basu Roy, Bill Bergeron, John Holodnak, et al. Ai-enabling workloads on large-scale gpu-accelerated system: Characterization, opportunities, and implications. In *2022 IEEE International Symposium on High-Performance Computer Architecture (HPCA)*, pages 1224–1237. IEEE, 2022.
- [29] Weile Luo, Ruibo Fan, Zeyu Li, Dayou Du, Qiang Wang, and Xiaowen Chu. Benchmarking and dissecting the nvidia hopper gpu architecture. *arXiv preprint arXiv:2402.13499*, 2024.
- [30] Pratyush Patel, Zibo Gong, Syeda Rizvi, Esha Choukse, Pulkit Misra, Thomas Anderson, and Akshitha Sriraman. Towards improved power management in cloud gpus. *IEEE Computer Architecture Letters*, 22(2):141–144, 2023.
- [31] Md Aamir Raihan, Negar Goli, and Tor M Aamodt. Modeling deep learning accelerator enabled gpus. In *2019 IEEE International Symposium on Performance Analysis of Systems and Software (ISPASS)*, pages 79–92. IEEE, 2019.
- [32] Prajit Ramachandran, Barret Zoph, and Quoc V Le. Searching for activation functions. *arXiv preprint arXiv:1710.05941*, 2017.
- [33] G Schieffer, D Medeiros, J Faj, A Marathe, and I Peng. Characterizing the performance, power efficiency, and programmability of amd matrix cores. Technical report, Lawrence Livermore National Laboratory (LLNL), Livermore, CA (United States), 2024.
- [34] Jaime Sevilla, Lennart Heim, Anson Ho, Tamay Besiroglu, Marius Hobbhahn, and Pablo Villalobos. Compute trends across three eras of machine learning. In *2022 International Joint Conference on Neural Networks (IJCNN)*, pages 1–8. IEEE, 2022.
- [35] Henry Cook SiFive. Diplomatic design patterns : A tilelink case study. 2017.
- [36] Wei Sun, Ang Li, Tong Geng, Sander Stuijk, and Henk Corporaal. Dissecting tensor cores via microbenchmarks: Latency, throughput and numeric behaviors. *IEEE Transactions on Parallel and Distributed Systems*, 34(1):246–261, 2022.
- [37] Seunghwan Sung, Sujin Hur, Sungwoo Kim, Dongho Ha, Yunho Oh, and Won Woo Ro. Mad macce: Supporting multiply-add operations for democratizing matrix-multiplication accelerators. In *Proceedings of the 56th Annual IEEE/ACM International Symposium on Microarchitecture*, pages 367–379, 2023.
- [38] Guangming Tan, Linchuan Li, Sean Triechle, Everett Phillips, Yungang Bao, and Ninghui Sun. Fast implementation of dgemm on fermi gpu. In *Proceedings of 2011 International Conference for High Performance Computing, Networking, Storage and Analysis*, pages 1–11, 2011.
- [39] Blaise Tine, Krishna Praveen Yalamarthy, Fares Elsabbagh, and Kim Hyesoon. Vortex: Extending the risc-v isa for gpgpu and 3d-graphics. In *MICRO-54: 54th Annual IEEE/ACM International Symposium on Microarchitecture*, pages 754–766, 2021.
- [40] Jiajun Wang, Ahmed Khawaja, George Biros, Andreas Gerstlauer, and Lizy K John. Optimizing gpgpu kernel summation for performance and energy efficiency. In *2016 45th International Conference on Parallel Processing Workshops (ICPPW)*, pages 123–132. IEEE, 2016.
- [41] Yang Wang, Chen Zhang, Zhiqiang Xie, Cong Guo, Yunxin Liu, and Jingwen Leng. Dual-side sparse tensor core. In *2021 ACM/IEEE 48th Annual International Symposium on Computer Architecture (ISCA)*, pages 1083–1095. IEEE, 2021.
- [42] Da Yan, Wei Wang, and Xiaowen Chu. Demystifying tensor cores to optimize half-precision matrix multiply. In *2020 IEEE International Parallel and Distributed Processing Symposium (IPDPS)*, pages 634–643. IEEE, 2020.
- [43] Xiuxia Zhang, Guangming Tan, Shuangbai Xue, Jiajia Li, Keren Zhou, and Mingyu Chen. Understanding the gpu microarchitecture to achieve bare-metal performance tuning. In *Proceedings of the 22nd ACM SIGPLAN Symposium on Principles and Practice of Parallel Programming*, pages 31–43, 2017.
- [44] Yunan Zhang, Po-An Tsai, and Hung-Wei Tseng. Simd2: A generalized matrix instruction set for accelerating tensor computation beyond gemm. In *Proceedings of the 49th Annual International Symposium on Computer Architecture*, pages 552–566, 2022.
- [45] Dan Zhao, Siddharth Samsi, Joseph McDonald, Baolin Li, David Bestor, Michael Jones, Devesh Tiwari, and Vijay Gadepally. Sustainable supercomputing for ai: Gpu power capping at hpc scale. In *Proceedings of the 2023 ACM Symposium on Cloud Computing*, pages 588–596, 2023.